46th AIAA Aerospace Sciences Meeting and Exhibit
7 - 10 January 2008, Reno, Nevada

AIAA 2008-68

Numerical Investigation of Oblique Fuel Injection in a Supersonic Combustor

A. Abdelhafez[*] and A. K. Gupta[†]
Department of Mechanical Engineering, University of Maryland
College Park, MD 20742

Oblique injection of fuel in a supersonic combustor has been investigated numerically in this study. The effects of important flow and injection parameters were substantiated and highlighted to assist in the development of an advanced supersonic combustor for hypersonic flight conditions. The parameters examined include airflow pressure and Mach number, fuel pressure and mass flow rate, and fuel injection angle. The results showed that static pressure of airflow is an important parameter governing mixedness in the oblique-injection flowfield. Higher pressures increased the resistance of airflow to penetration. Thus, the fuel flow was confined to a thinner boundary layer that mixed up faster with air due to subsequent shock/shear layer interactions. Moreover, air Mach number did not govern the quality of air-fuel mixing, i.e., increasing air Mach number does not necessarily result in better mixing. Increasing the fuel pressure (mass flow rate) at constant airflow was observed to result in deeper penetration but at the expense of both fuel system efficiency and effectiveness. Changing the injection angle (limited to small angles of up to about 20°) was found not to affect the flowfield significantly. A comparison was performed between the flowfields of an oblique- and a traverse-injection port. The flowfield of the former is entirely supersonic and free of large-scale streamwise vorticity fields, unlike that of the latter. The results obtained on mixing under non-reacting conditions assist in providing good insights on the oblique-injection configuration in pursuit of better mixing with lower losses and higher thrust.

I. Introduction

Scramjet-engine-powered vehicles are the future of high-speed flight. Nevertheless, mixing and ignition in such engines still need extensive investigation, in order to achieve full understanding of the complicated flow dynamics and chemistry involved. Successful operation of any air-breathing system depends on efficient mixing, ignition, and combustion.[1] The efficiency and effectiveness of an injection system are defined by the degree of fuel/air mixing and the system capability of minimizing injection-induced thrust losses, respectively.[2] Over a considerable part of the vehicle flight, the equivalence ratio of operation has to be fuel-rich to ensure that a flame is present to provide positive thrust. Therefore, any progress made on improving the scramjet engine efficiency must be closely followed towards achieving efficient mixing between fuel and air. Scramjet flows have residence times of the order of only few milliseconds. Within that short residence time, the mixing, ignition delay, and combustion time scales should be accounted for.

Figure 1 shows a simplified chemical kinetics analysis that sheds some light on this technical challenge. Plotted are the temporal variations of temperature for hydrogen/air mixtures of different equivalence ratios inside a plug-flow reactor. Fuel-rich conditions are considered, as is the case for actual scramjet operation. Perfect mixing is assumed, i.e., hydrogen mixes instantaneously and homogeneously over the entire reactor cross-section after injection. The inlet air temperature and Mach number are chosen to be 1000 K and 4.0, respectively, as common representatives of the conditions after the inlet and isolator sections of a hypersonic vehicle. The air temperature is assumed not to change due to fuel injection. Constant combustor pressure is assumed throughout at 1 atm. It can be seen from Figure 1 that the ignition delay increases from 0.25 to 1.2 ms with increase in equivalence ratio. The average value of ignition delay agrees well with the findings of previous research.[3,4,5] If the assumption of perfect mixing is relieved, the mixing time scale and mixture non-homogeneity will have to be accounted for. This imposes more challenges, if a target residence time of few milliseconds is sought. Failure to meet such strict demands reflects on the combustor length, which, in turn, affects the vehicle weight, available payload, developed thrust, and specific impulse.

Previous research has shown that flame holding in reacting supersonic flows is achieved by creating high-vorticity regions, where fuel and air partially mix at lower velocities.[6] In case of traverse fuel injection from a wall orifice, a bow shock is formed as a result of the interaction of fuel jet and supersonic crossflow of air, see Figure 2. Consequently, the upstream wall boundary layer separates, providing a region where the boundary layer and fuel jet mix subsonically upstream of the jet exit. It was reported that this region is important in the traverse-injection flowfield because of its flame-holding capability under reacting conditions. Several

[*] Graduate Student, Student Member AIAA
[†] Professor, Fellow AIAA, email: akgupta@umd.edu

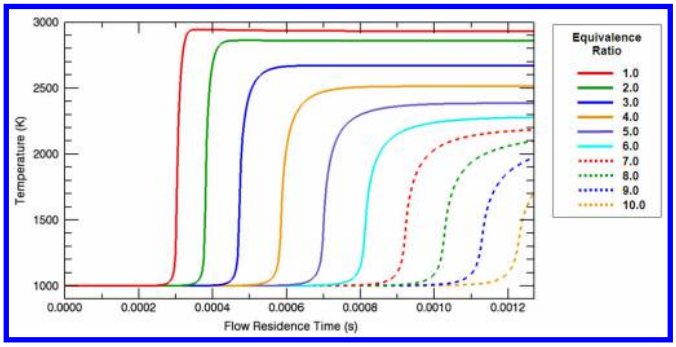

Figure 1. Temporal temperature variation of a perfectly-stirred, constant-pressure, plug-flow H_2/air reactor. Initial air temperature and Mach number = 1000 K and 4.0, respectively, reactor pressure = 1 atm.

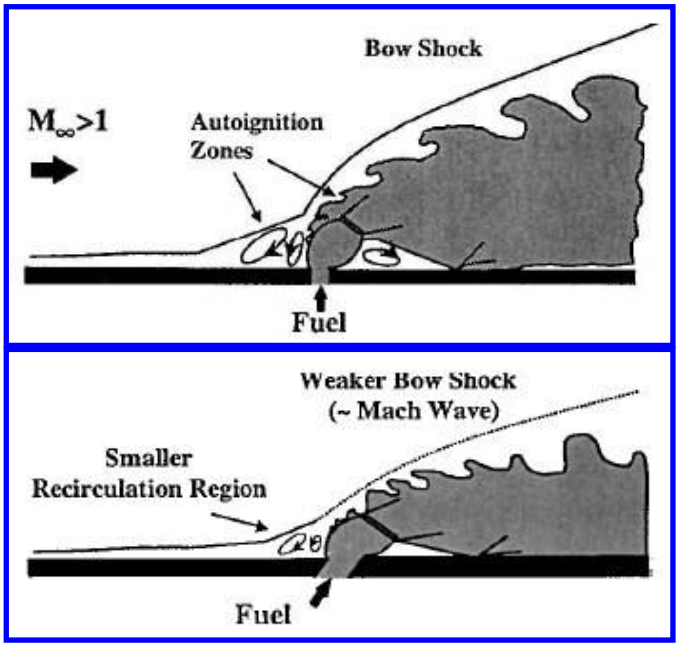

Figure 2. Traverse (top) and oblique injection (bottom), [6]

studies have been conducted on this region.[7,8] Autoignition was observed at the jet upstream recirculation region and behind the bow shock. However, this injection configuration does not provide the desired full penetration of fuel into the supersonic crossflow of air. Furthermore, it has significant stagnation pressure losses due to the strong three-dimensional bow shock[9] formed by the traverse jet penetration. On the other hand, it is possible to increase the injection system effectiveness, i.e., reduce the injection-induced total pressure losses, by using angled (oblique) injection. A weaker shock results, see Figure 2. In this configuration, the fuel jet axial momentum can also contribute to the net engine thrust.

Fuel injection at small oblique angles was preferred to traverse injection in different experimental studies.[10,11] The combustion of gaseous hydrogen fuel injected from a hyper-mixer at 12° and 17° in a Mach-3.0 airflow was investigated. Whereas oblique injection maintained a supersonic combustion environment, traverse injection yielded subsonic combustion, which is not favorable in scramjet engine operation, due to the large accompanying bow-shock losses. The results showed that the oblique shock waves, generated by the hyper-mixer, induce an environment suitable for operating the combustor in the supersonic mode. This owes to the ability of oblique shock waves for supersonic mixing enhancement and preventing large-scale boundary layer separation. Moreover, the oblique shocks provide a means for near-field flameholding.

The oblique configuration of fuel injection was also compared to the traverse one in a numerical study.[5] A Mach-2.35 combustor was considered, with oblique injection performed at 5°. It was concluded that oblique injection at small angles is recommended, as it provides superior performance from the points of fuel system efficiency and effectiveness, flow blockage, and boundary layer separation.

In another experimental investigation,[12] a supersonic hydrogen flame, with coaxial injection, was stabilized successfully along the axis of a Mach 2.5 wind tunnel. Stabilization was achieved by using small-angled wedges mounted on the tunnel sidewalls to generate weak oblique shock waves that interact with the flame. It was found that these shock waves enhance fuel-air mixing to the extent that the flame length decreased by up to 30%, when certain shock locations and strengths were chosen that are optimum for the investigated geometry and operating conditions. The researchers reasoned that enhanced mixing resulted, in part, because the shocks induce radial inflows of air into the fuel jet. It was concluded that optimizing the mixing and stability limits for any combustor geometry requires careful matching of shock strengths and locations of shock/flame interaction.

In another investigation[13] shock-induced mixing was simulated numerically. Parallel flows of a heavy gas interspersed with other flows of a lighter one were overtaken by a normal shock wave. It was shown that vorticity is generated at each location of interaction of the density gradient across each light/heavy interface with the shock wave pressure gradient. Since the pressure and density gradient vectors are out of phase at these locations, their cross-product ($\nabla p \times \nabla \rho$) has non-zero values. This cross-product defines the Baroclinic vorticity vector, $\partial_t \vec{\omega}_{bc} = (\nabla p \times \nabla \rho)/\rho^2$, which causes the light gas regions to roll up into one or more counter-rotating vortex pairs, stirring and mixing the light and heavy gases together. It was concluded that, whenever possible, multiple shock waves should be utilized.

Shock waves of supersonic flows have significant positive effects on fuel-air mixing and flame stabilization, when they interact appropriately with the air/fuel shear layer. Some beneficial effects of this interaction[14] are: (a) directing the airflow locally towards fuel for increased entrainment rates, (b) creation of additional vorticity that enhances mixing, (c)

elongation of the flame recirculation zones due to the adverse pressure gradient of a shock wave, and (d) increasing the flow static pressure and temperature through a shock wave. The exact role of each effect needs further substantiation and quantification. This present work has the objective of numerically investigating oblique fuel injection in a supersonic combustor. Different flow and injection parameters are examined for their individual effects on fuel system efficiency and effectiveness. These parameters include air static pressure and Mach number, fuel pressure and flow rate, and injection angle. Air flow rate was investigated in similar previous work.[5] The goal is to achieve enhanced mixing while reducing injection-induced pressure losses.

II. Test Matrix and Simulation Assumptions

Since numerical approach is used here, code validation and comparisons to actual experimental data were facilitated by choosing the Mach-2.35 combustor of the experimental work of Balar et al.[15] The geometry of this combustor is depicted here in Figure 3a. The traverse-injection port was replaced by an oblique-injection one.

Air is supplied from a 5.1-cm pipe and accelerated subsonically through a convergent section to a square cross-sectional area of 1.27 x 1.27 cm^2. This 1.27-cm spanwise dimension of the flow passage maintains this value up to the test rig exit plane. The airflow is then further accelerated through a convergent-divergent (CD) nozzle. A quadrant of a disc 0.518 cm in diameter and 1.27 cm thick (i.e., spanning the entire flow passage) forms the convergent section of this nozzle, which results in a rectangular flow throat area of 0.752 x 1.27 cm^2. The nozzle divergent section was designed using the method of characteristics and expands the flow back to an area of 1.27 x 1.27 cm^2. The flow passage upper and lower walls then expand at 3.5° each for an axial distance of 3.8 cm to further accelerate the flow to a Mach number of 2.35, keeping the spanwise dimension constant at 1.27 cm. This expansion section is marked green on Figure 3a. Following the expansion is a fuel injection section, where the flow passage maintains a constant area of 1.735 x 1.27 cm^2 for 3.18 cm and terminates by the 0.318-cm injection port. To prevent choking and/or excessive blockage of the airflow, due to fuel injection, the upper and lower walls of flow passage expand again, right after the injection port, at 3.5° each for 28.56 cm up to the test rig exit plane.

To facilitate the ability of changing the air Mach number at the location of fuel injection, the dimensions of the post-nozzle expansion section (marked green on Figure 3a) were altered, yielding two additional combustor geometries. That section was eliminated completely to provide a Mach-2.0 combustor (Figure 3b), and extended by a factor of 2.4 to provide a Mach-2.7 combustor (Figure 3c). Throughout this study, the three combustors of Figures 3a – 3c will be designated as medium-, low-, and high-Mach combustors, respectively.

The ESI-Group CFD-FASTRAN 2007 LES-based code was used for all simulations presented here. A variable-sized grid was generated for the examined geometry with a total of 284284, 258258, and 309972 nodes for the medium-, low-, and high-Mach combustors, respectively. Tighter meshing was implemented near and at the critical geometry locations, e.g., convergent-divergent nozzle, fuel injection port, and corners of expansion. Special emphasis was placed on the level of cell skewness. The flow passage was divided into six sub-volumes of regular geometrical shapes (i.e., pyramid frustums and parallelepipeds), with each volume meshed separately, in order to keep the skewness level of the most skewed cell below 0.5.

The Baldwin-Lomax turbulence model was implemented. Calculation of viscosity and conductivity was based on the kinetic theory of gases. The mass diffusivity was calculated based on Fick's law with a Schmidt number of 0.5. A turbulent Prandtl number of 0.9 was used for calculating the turbulent conductivity. The total pressure and temperature at the air inlet were kept fixed at 300 K and 6.44 bar, respectively. Thus, these two quantities of the air inlet were preserved throughout the iteration process in each examined case, until convergence was attained. Consequently, all analyses of this study have a common air flow rate of 146 g/s. Owing to the relatively large cross-sectional area of the air inlet, the entrance velocity of air was only 9.4 m/s, resulting in almost identical inlet stagnation and static conditions. Fuel was simulated with helium, similar to that used experimentally by Balar et al.[15] Two mass flow rates of helium are investigated, namely 1.98 and 4.26 g/s. For both flow rates, the speed of injection is sonic, 883 m/s, at a total temperature of 300 K. Thus, the amount of injected helium is controlled solely by the injection total pressure of 2.700 and 5.762 bar abs, respectively. The nozzle walls were set to be adiabatic, assuming insignificant heat transfer through the thick test rig walls.

The initial conditions of simulation were set equal to those of the air inlet for each case, i.e. velocity of 9.4 m/s and static temperature of 300 K. The static pressure, however, was set to 1 atm. Consequently, the simulation incorporated the transient flow behavior once the air supply valve is opened in the experimental test facility, allowing the high-pressure air to expand and "march" from inlet to exit. A total of 9000 iterations or cycles were set for each simulated case. Convergence was usually attained after 8000 – 8500 iterations.

Table 1 lists the test matrix for the simulation results presented here. For constant air mass flow rate and inlet total pressure and temperature, this study focuses on highlighting the individual effects of the following parameters on the fuel system efficiency and effectiveness within the oblique-injection configuration:

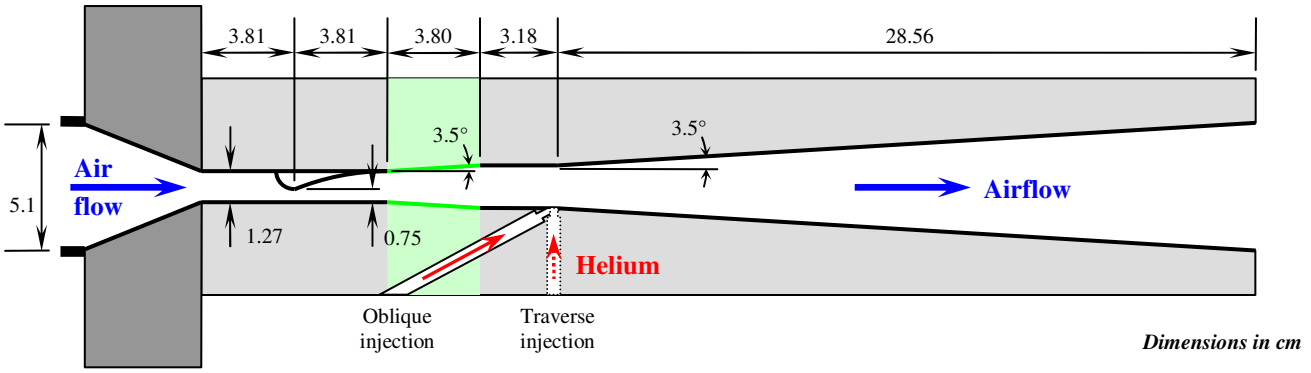

Figure 3a. Schematic of the Mach-2.35 combustor

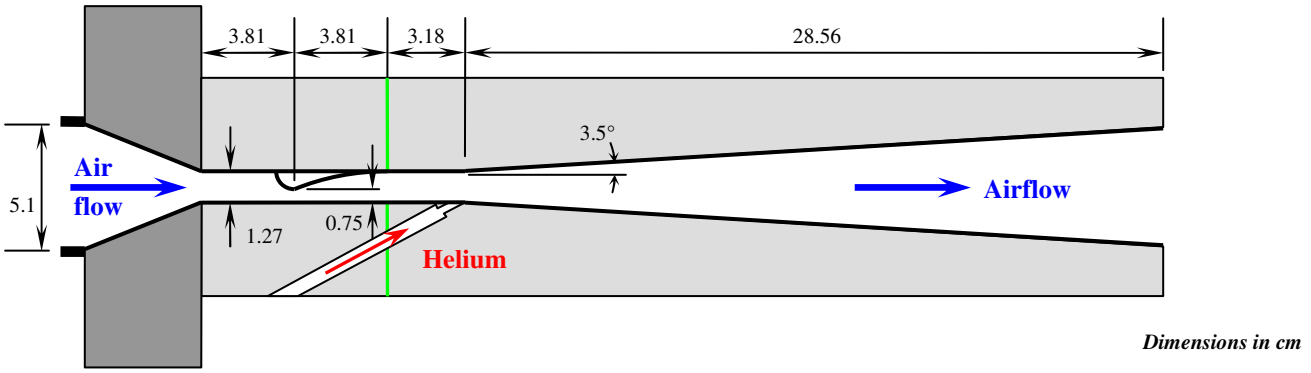

Figure 3b. Schematic of the Mach-2.0 combustor (post-nozzle expansion section absent)

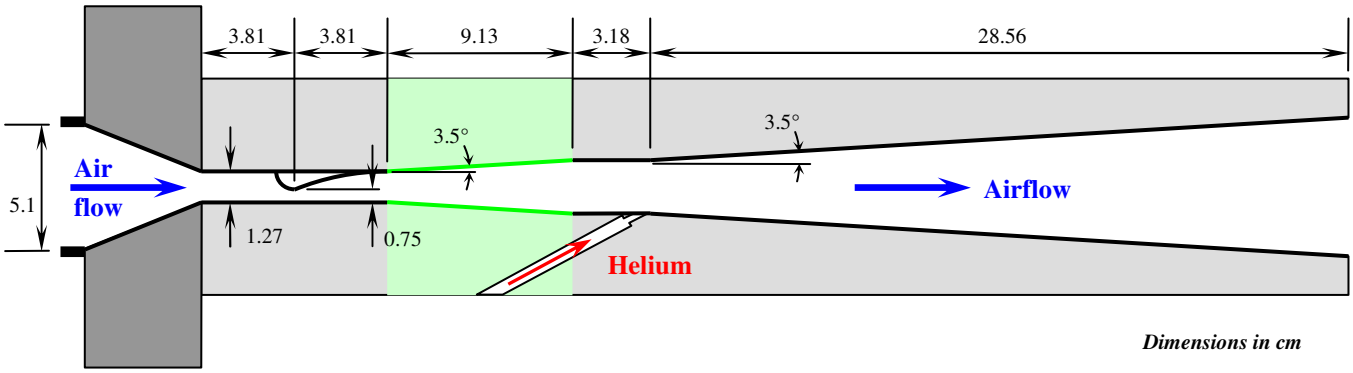

Figure 3c. Schematic of the Mach-2.7 combustor (post-nozzle expansion section extended)

- Air Mach number, with values of 2.0, 2.35, and 2.7,
- Fuel pressure (mass flow rate), with values of 2.7 and 5.762 bar (1.98 and 4.26 g/s), and
- Fuel injection angle, with values of 3°, 5°, 7°, and 10°.

The effects of air pressure and flow rate were investigated in similar previous work[5] on the geometry of the medium-Mach combustor (Figure 3a). Nevertheless, these effects will be reviewed here in order to attain a comprehensive analysis of oblique fuel injection in supersonic airflows.

III. Results and Discussion

Code Validation

A sample code-validation comparison is depicted in Figure 4. Shown is the variation in static pressure along the flow passage upper wall (opposite to the fuel injection port). The medium-Mach combustor is considered with traverse helium injection, air inlet total pressure and temperature of 6.44 bar and 300 K, respectively, and helium pressure (flow rate) of

Table 1. Test Matrix

Air total pressure at inlet = 6.44 bar (constant)
Air total temperature at inlet = 300 K (constant)
Air mass flow rate = 146 g/s (constant)

Case No.	Air Mach number	Helium total pressure [bar] / mass flow rate [g/s]	Injection angle [deg]
1	2.0	2.7 / 1.98	3
2			5
3			7
4			10
5		5.762 / 4.26	3
6			5
7			7
8			10
9	2.35	2.7 / 1.98	3
10			5
11			7
12			10
13		5.762 / 4.26	3
14			5
15			7
16			10
17	2.7	2.7 / 1.98	3
18			5
19			7
20			10
21		5.762 / 4.26	3
22			5
23			7
24			10

2.7 bar (1.98 g/s). The wall static pressure values are normalized by the total pressure at the air inlet, while the axial location is normalized by the injection-port diameter (d = 0.318 cm). Good agreement is observed between the numerical and experimental results.

The development of a non-intrusive diagnostic technique for in-situ mixture fraction quantification based on the principles of absorption spectroscopy is currently underway.[16] The mixture fraction data will allow for further validation of the numerical results, in addition to our work on the static pressure measurements along the combustor upper wall.

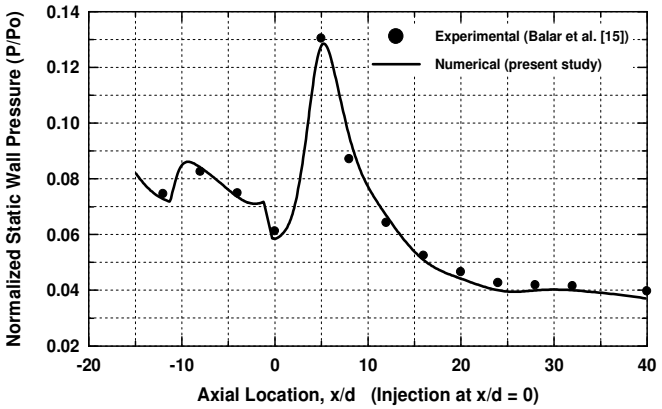

Figure 4. Static pressure variation along the flow passage upper wall (opposite of fuel injection port); pressure normalized by total pressure at air inlet (6.44 bar); axial location normalized by injection-port diameter (d = 0.318 cm). Helium pressure (mass flow rate) = 2.7 bar (1.98 g/s).

Effect of Air Mach Number

In order to examine the effect of air Mach number, cases 2, 10, and 18 of low-, medium-, and high-Mach combustors, respectively, are compared to each other in Figure 5. Presented are the center-plane profiles of Mach number, fuel (helium) mass fraction, and static pressure profiles in Figures 5a, 5b, and 5c, respectively. Those three cases differ in combustor Mach number but have a common fuel pressure (mass flow rate) of 2.7 bar (1.98 g/s) and injection angle of 5°. Aside from the obvious fact that the average Mach number increases with ascending case number, it is worth noting that all three cases have very similar shock structures.

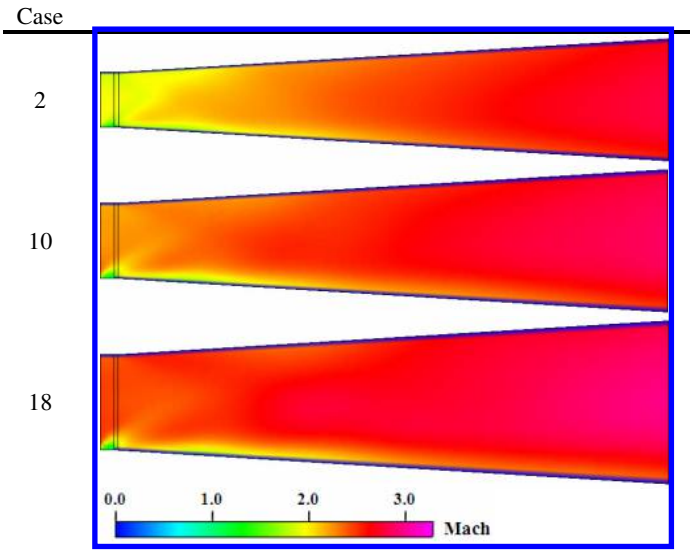

Figure 5a. Mach number profiles at the center plane within the first 40 injection-port diameters downstream of the injection point for cases 2 (low-Mach), 10 (medium-Mach), and 18 (high-Mach). Helium pressure (mass flow rate) = 2.7 bar (1.98 g/s). Injection angle = 5°.

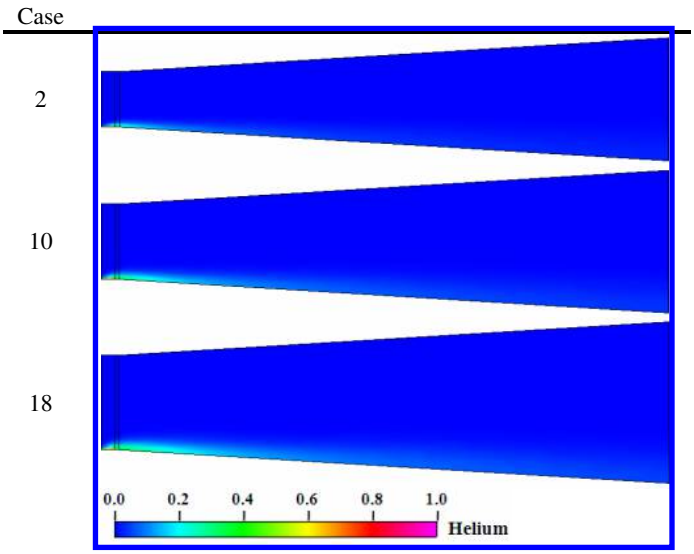

Figure 5b. Helium mass fraction profiles at the center plane within the first 40 injection-port diameters downstream of the injection point for cases 2 (low-Mach), 10 (medium-Mach), and 18 (high-Mach). Helium pressure (mass flow rate) = 2.7 bar (1.98 g/s). Injection angle = 5°.

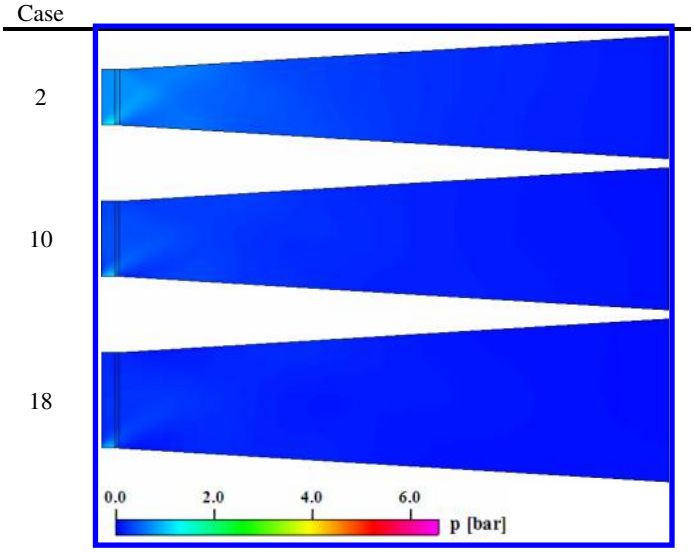

Figure 5c. Static pressure profiles at the center plane within the first 40 injection-port diameters downstream of the injection point for cases 2 (low-Mach), 10 (medium-Mach), and 18 (high-Mach). Helium pressure (mass flow rate) = 2.7 bar (1.98 g/s). Injection angle = 5°.

Since the deflection angle, induced by the injected fuel jet, is kept constant at 5°, a decrease in the angle of the injection-port shock wave was expected, as the air Mach number is increased. Different shock angles result in significantly different shock structures downstream of the injection port, as the shocks reflect off the air/fuel shear layer and combustor walls. The same shock angle is observed in Figure 5a, which results in almost identical shock structures for all three cases. Other important observations, to be made from Figure 5b, are that (a) the fuel mixedness deteriorates and (b) the penetration increases, as the air Mach number is increased. Both observations negate the common expectations of better mixedness and less penetration at higher air Mach numbers. A plausible explanation for these unique findings can be obtained from Figure 5c, where the static pressure profiles are depicted. Since the static pressure and Mach number of any flow are inversely proportional at constant total pressure, higher average static pressures were expected at lower Mach numbers. Thus, it can be concluded from the helium mass fraction profiles of Figure 5b that fuel mixedness and penetration are dominated by the air static pressure and not the Mach number. Higher static pressures increase the ability of airflow to resist penetration and suppress the fuel flow to thinner boundary layers that get consumed faster by subsequent shock/shear layer interactions. The fact that fuel mixedness enhances at higher static pressures is beneficial for scramjet operation. As the flight speed of a hypersonic vehicle increases, the total pressure of the incoming airflow also increases. If the average combustor Mach number is to be maintained roughly constant, the static pressure inside the combustor will have to increase, which results in better fuel mixedness according to the above analysis. The findings of this analysis agree well with those of previous research,[5] where it was shown that increasing the air mass flow rate (which is indicative of higher flight speeds) increases the air static pressures inside the combustor at a roughly constant Mach number, resulting in better mixedness for the same fuel flow rate. It should be noted, however, that increasing the flight speed requires more thrust production, which can only be achieved by injecting more fuel. Thus, changes in fuel flow rate should be accounted for, as the following section explains.

Effect of Fuel Pressure / Flow Rate

The effect of fuel pressure (mass flow rate) is highlighted in Figure 6. For each of the three considered combustors two fuel pressures (mass flow rates) are examined, namely 2.7 bar (1.98 g/s) and 5.762 bar (4.26 g/s). Figure 6a shows the Mach number profiles at the center plane within the first 40 injection-port diameters downstream of the injection point. Figure 6b, on the other hand, shows the corresponding helium mass fraction profiles.

It can be clearly observed that, keeping all other parameters constant, increasing the fuel pressure (mass flow rate) results in deeper penetration at the expense of fuel system efficiency and effectiveness. This was expected, as higher fuel pressures imply higher energy of the fuel jet and, consequently, an increased ability to penetrate the airflow to greater depths. However, fuel system efficiency and effectiveness are sacrificed. Longer axial distances are needed downstream of the injection port to consume the fuel-rich layer near the bottom combustor wall. Moreover,

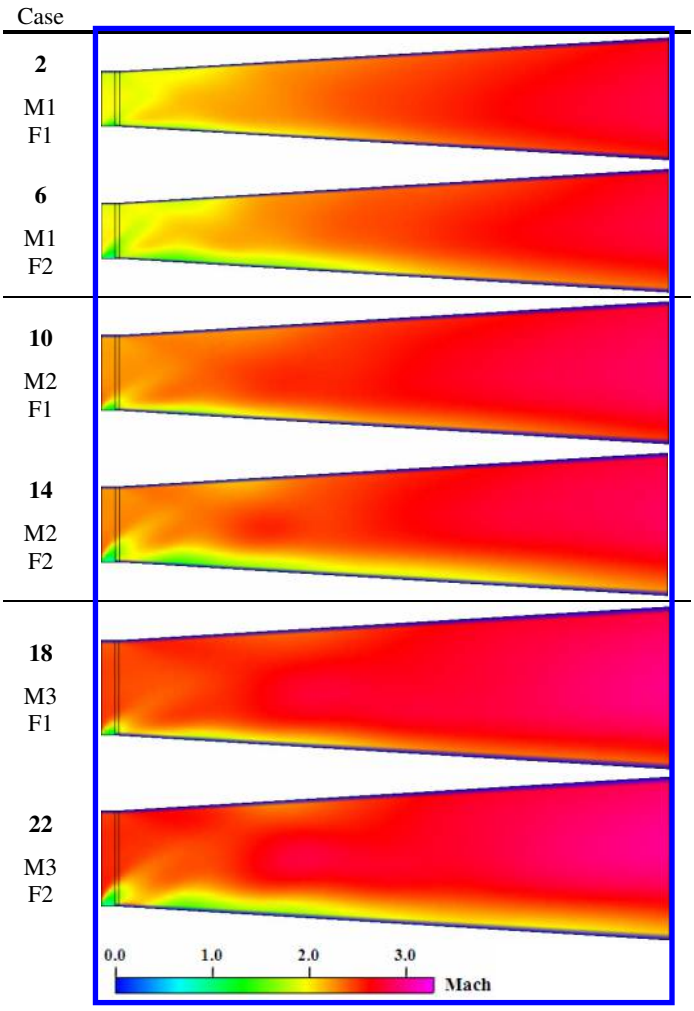

Figure 6a. Mach number profiles at the center plane within the first 40 injection-port diameters downstream of the injection point. Injection angle = 5°. M1 ≡ low-Mach, M2 ≡ medium-Mach, M3 ≡ high-Mach. F1 ≡ fuel pressure (mass flow rate) = 2.7 bar (1.98 g/s), F2 ≡ fuel pressure (mass flow rate) = 5.762 bar (4.26 g/s).

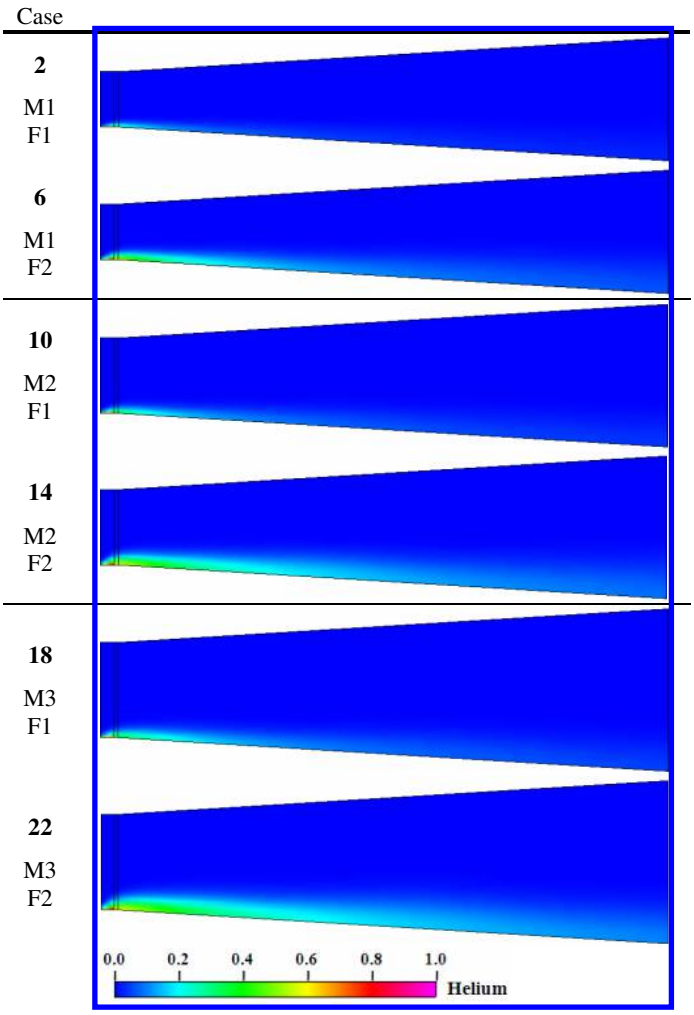

Figure 6b. Helium mass fraction profiles at the center plane within the first 40 injection-port diameters downstream of the injection point. Injection angle = 5°. M1 ≡ low-Mach, M2 ≡ medium-Mach, M3 ≡ high-Mach. F1 ≡ fuel pressure (mass flow rate) = 2.7 bar (1.98 g/s), F2 ≡ fuel pressure (mass flow rate) = 5.762 bar (4.26 g/s).

the injection-induced shock train gains strength without any significant positive effects on mixing, i.e., only the negative effects of shock formation prevail in form of increased total pressure losses. These findings agree well with those of previous research,[5] where it was shown that increasing the fuel flow rate at constant airflow and injection angle yields deeper penetration with poorer fuel system performance.

It is worth noting at this point that a sub-comparison of cases 6, 14, and 22 of Figure 6 reveals the same results obtained earlier in the analysis of the effect of air Mach number. Increasing the airflow Mach number does not yield better mixing. This is again attributed to the fact that the air static pressure is the key parameter governing the quality of mixing, where higher pressures suppress the fuel to a thinner layer that gets consumed faster through the increased efficiency of shock/shear layer interaction.

Effect of Injection Angle

The effect of injection angle is highlighted in Figures 7a and 7b, which show the center-plane Mach number and helium mass fraction profiles within the first 40 injection-port diameters downstream of the injection point of the medium-Mach combustor. Helium pressure and mass flow rate are kept constant at 5.762 bar and 4.26 g/s, respectively.

The results show that changing the injection angle within the narrow window of recommended small angles does not affect the flowfield significantly. As the injection angle is increased, the injection-port shock wave gains strength slightly, and the fuel jet manages to penetrate the airflow somewhat more. A small drop in fuel mixedness occurs in the near field, whereas far-field mixing is hardly affected. Figure 8 magnifies the small differences in near-field mixing

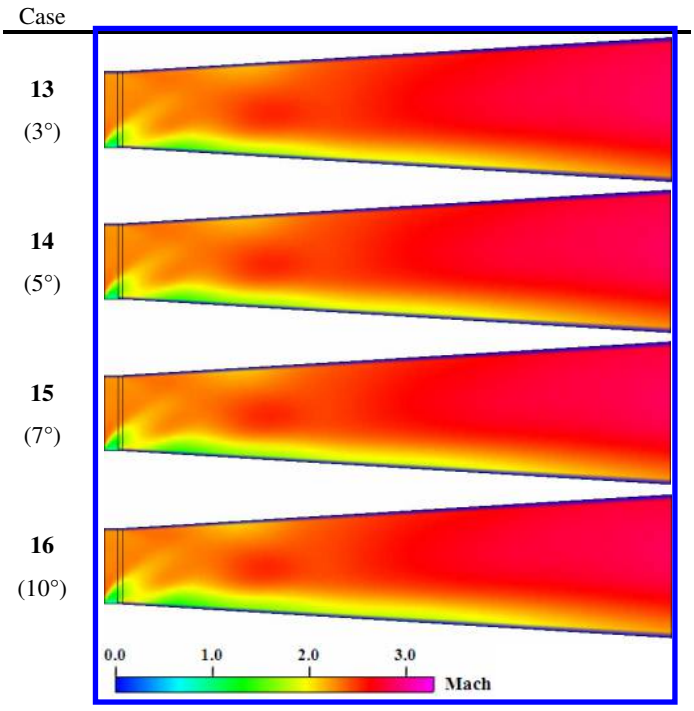

Figure 7a. Center-plane Mach number profiles within the first 40 injection-port diameters downstream of the injection point of the medium-Mach combustor. Helium pressure (mass flow rate) = 5.762 bar (4.26 g/s).

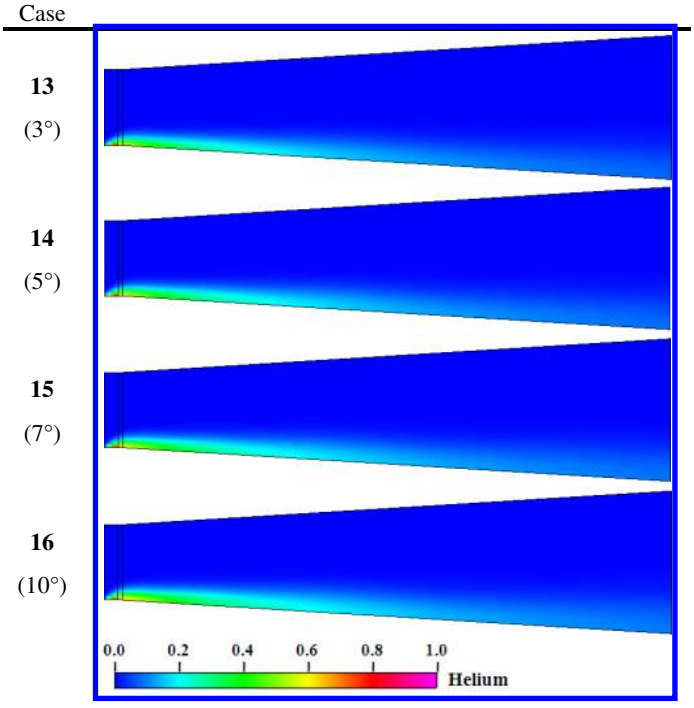

Figure 7b. Center-plane helium mass fraction profiles within the first 40 injection-port diameters downstream of the injection point of the medium-Mach combustor. Helium pressure (mass flow rate) = 5.762 bar (4.26 g/s).

between the four cases of Figure 7 for a clearer presentation. Such differences peak at an axial location of x/d ≈ 10 but vanish rapidly, as the flow advances axially. It should be noted that cases 13 to 16 are not the single group of cases where the described effect of injection angle is identifiable. All 24 cases listed in Table 1 demonstrate these trends, when compared against each other for the effect of injection angle. A summary of the Mach number and helium mass fraction center-plane profiles of all cases examined here is shown in Table 2.

Flowfields under Oblique and Traverse Injection

Previous research[9] on traverse injection in supersonic flows studied the flowfield structure at and downstream of the traverse-injection port, as depicted in Figure 9. In the shadow of a strong three-dimensional bow shock, the injected fuel jet propagates subsonically surrounded by a subsonic air/fuel shear layer and a subsonic envelope of airflow. This allows the fuel jet boundary and air/fuel shear layer to remain smooth without any significant disturbances or corrugations for a considerable distance downstream of the injection port, as shown in Figure 9. The subsonic nature of the fuel jet and adjacent airflow also allows for large-scale streamwise counter-rotating vortices to develop and propagate, thus assisting in air-fuel mixing. Moreover, the higher penetration accompanying traverse injection allows the fuel flow to propagate away from the combustor bottom wall, confining a thick boundary layer underneath it. The average flow Mach number within this boundary layer is considerably lower than that of the main flow, which allows for boundary layer separation and creation of recirculation zones at the bottom wall.

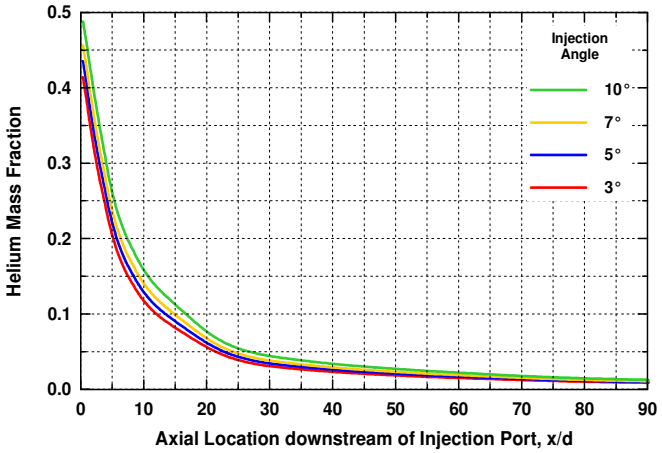

Figure 8. Variation of helium mass fraction at the intersection line of the central plane with the bottom wall of the medium-Mach combustor. Helium pressure (mass flow rate) = 5.762 bar (4.26 g/s). Axial location normalized by injection-port diameter (d = 0.318 cm).

Table 2. Center plane profiles within the first 40 injection-port diameters downstream of the injection point for all cases listed in Table 1

Air total pressure and temperature at inlet = 6.44 bar and 300 K (constant)
Air mass flow rate = 146 g/s (constant)

Mach Number

	Case	Fuel pressure (mass flow rate) = 2.7 bar (1.98 g/s)	Case	Fuel pressure (mass flow rate) = 5.762 bar (4.26 g/s)
		Low-Mach combustor (M = 2.0)		
3°	1	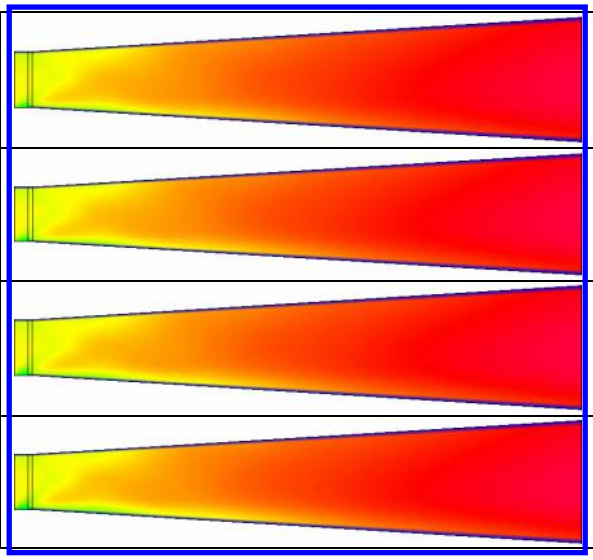	5	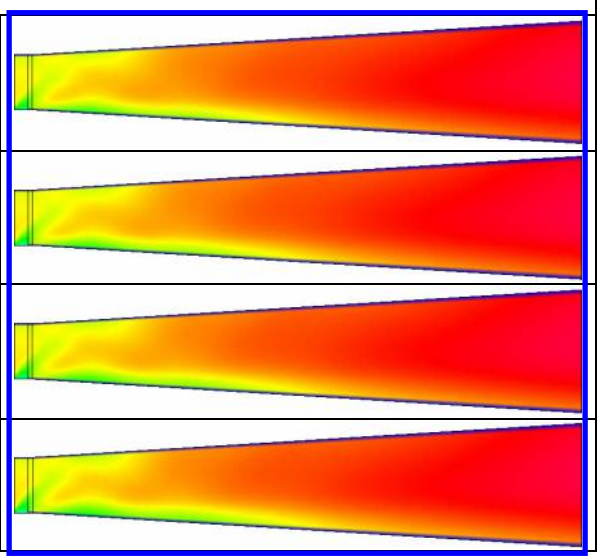
5°	2		6	
7°	3		7	
10°	4		8	
		Medium-Mach Combustor (M = 2.35)		
3°	9	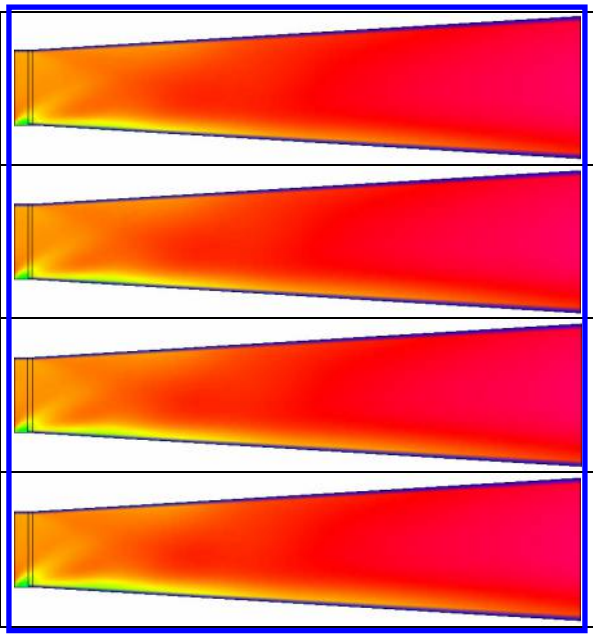	13	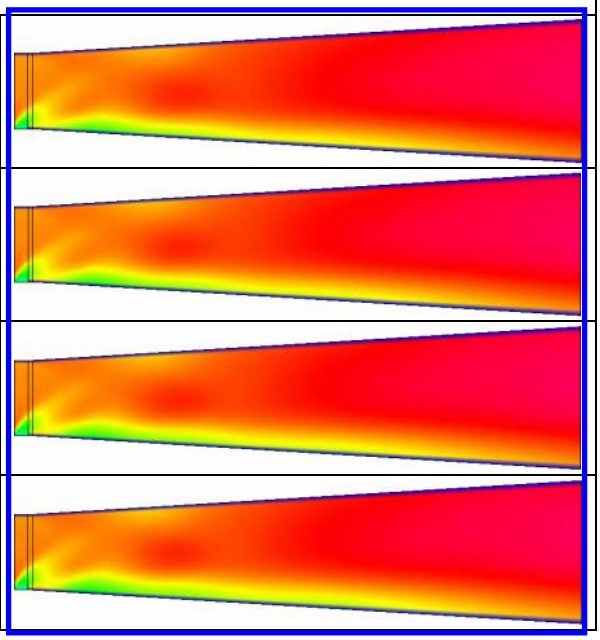
5°	10		14	
7°	11		15	
10°	12		16	

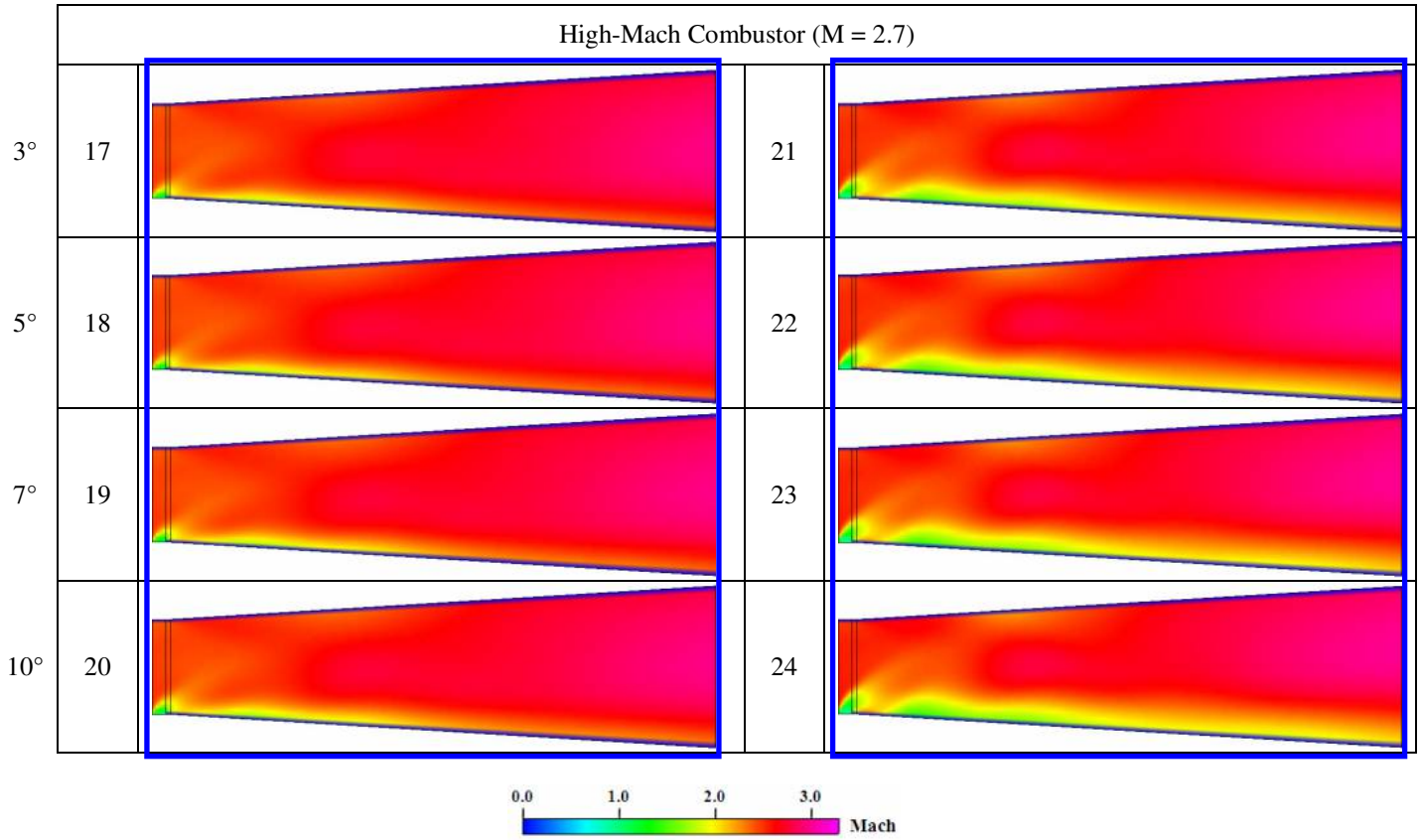

Helium Mass Fraction

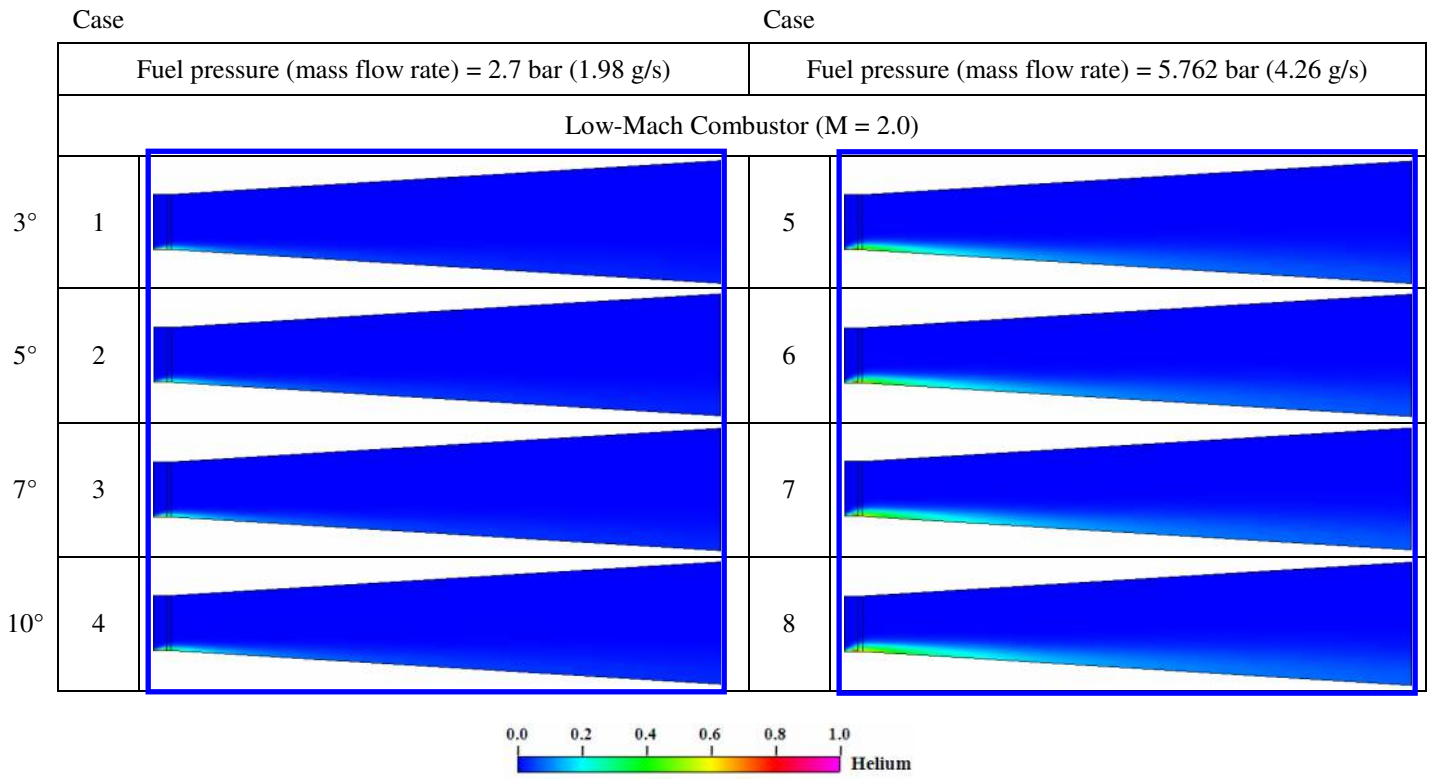

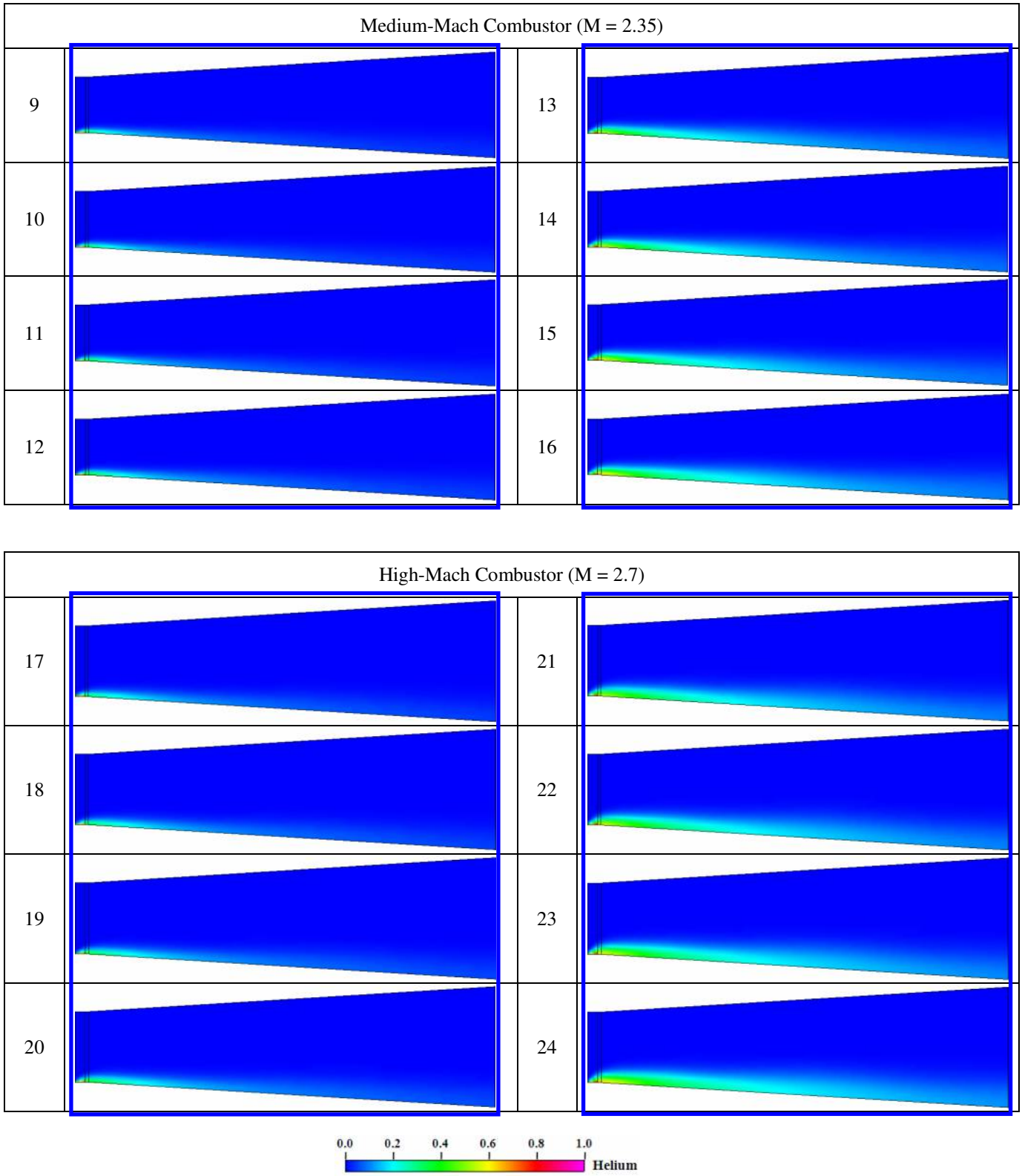

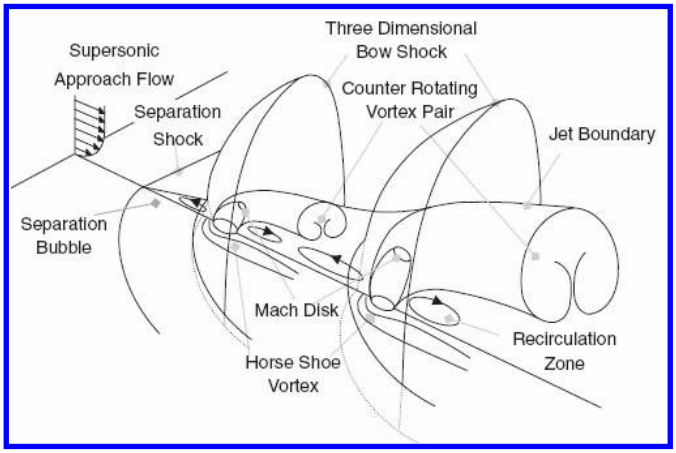

Figure 9. Schematic view of mean flowfield of dual transverse injection [9]

To avoid any discrepancies due to the use of different numerical codes or geometries in Ref. [9] and this study, traverse injection was simulated in the medium-Mach (M = 2.35) combustor at a fuel pressure (mass flow rate) of 5.762 bar (4.26 g/s). Figure 10 shows the Mach number profiles downstream of the injection port for the resulting flowfield. Seven selective cross-sectional areas or stations were chosen for display in an isometric view of the combustor. The center-plane view is also depicted with the projections of these seven stations indicated. Blue arrows on the isometric view indicate significant directions of local flow.

The following observations can be made form the center-plane profile in Figure 10. A strong bow shock is formed upstream of the injection port. The strength of this shock wave is high enough to reduce the maximum Mach number of the traverse-injection flowfield down to 2.8, as compared to an average value of 3.3 for all oblique-injection cases of this study. This drop in maximum Mach number implies higher total pressure losses and lower fuel system effectiveness. A considerable stand-off distance exists between the bow shock and injection port, allowing for an upstream recirculation region, similar to what was reported in previous literature.[6] The angle and strength of the bow shock at the combustor top wall remain significantly high, resulting in a reflection with detachment. Deep penetration is achieved. Thus, the fuel flow propagates away from the combustor bottom wall, with a thick boundary layer underneath it. The average flow Mach number within this boundary layer is considerably lower than that of the main flow. Two distinct boundary layer separation and flow recirculation zones exist at the bottom wall.

The existence of a large-scale stream-wise vorticity field is observed in the isometric view in Figure 10. As the arrow on station 2 shows, a region of higher Mach number commences at the combustor back wall away from the center plane, which was not evidenced before in station 1. This region develops from stations 2 to 3. After the flow adjusts its direction at the detached-shock reflection (station 4), the

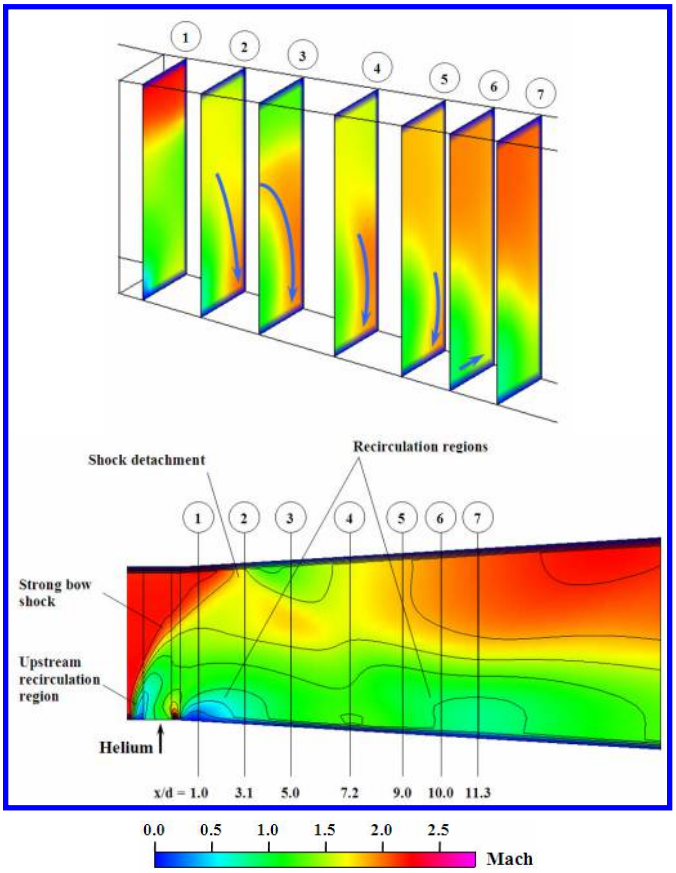

Figure 10. Mach number profiles downstream of injection port for a traverse-injection flowfield (M = 2.35, fuel pressure = 5.762 bar). Top: Isometric view of seven selective cross-sectional areas; bottom: center-plane view with the projections of these seven cross-sectional areas indicated. Blue arrows indicate significant directions of local flow.

region of higher Mach number shrinks (stations 4 to 5) and eventually vanishes at station 6, as the downstream recirculation region commences. To adapt for the existence of the recirculation region at the bottom wall near the center plane, the fuel jet expands in the spanwise direction (see direction of arrow at station 6 in Figure 10).

It can be clearly seen at this point that the traverse-injection flowfields of Ref. [9] and this study show direct matches in all major aspects with some minor differences due to confinement. Implementing oblique injection, on the other hand, results in a flow structure, which has some common features with that of traverse injection, yet differs in some other substantial aspects. Repeating the analysis of Figure 10 under the same conditions of air Mach number (M = 2.35) and fuel pressure (5.762 bar) but with oblique injection at 3° results in the flowfield depicted in Figure 11. It starts with a three-dimensional oblique shock wave at the injection port (station 1) similar in shape to the bow shock of traverse injection, but of smaller strength (since the flow remains supersonic). The pressure rise, imposed by this shock wave

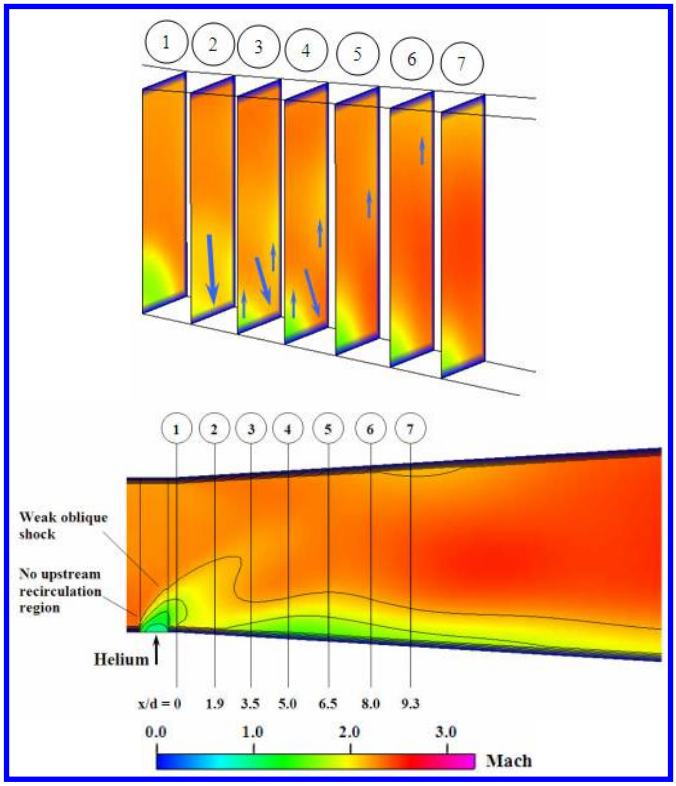

Figure 11. Mach number profiles downstream of injection port for an oblique-injection flowfield (M = 2.35, fuel pressure = 5.762 bar, injection angle = 3°). Top: Isometric view of seven selective cross-sectional areas; bottom: center-plane view with the projections of these seven cross-sectional areas indicated. Blue arrows indicate significant directions of local flow.

on the flow, gives the airflow a negative velocity component in the lateral direction (blue arrow on station 2), thus the fuel flow gets suppressed to a thinner layer adjacent to the bottom wall. This act of suppression increases the pressure of fuel flow, which resists being suppressed by gaining a positive lateral velocity component (small upward arrow on the left side of station 3). Consequently, the airflow adapts by gaining a component in the spanwise direction (tilting of downward arrow on station 3). This spanwise adaptation is known as the three-dimensional relief effect. As a result of the spanwise adjustment, the part of airflow adjacent to the back wall of the combustor adapts, in turn, by acquiring a positive lateral velocity component (small upward arrow on the right side of station 3). This trend prevails until the flow fully develops at station 7.

It is worth noting here that these lateral movements of air and fuel flows can be considered as the "supersonic version" of the subsonic flowfield downstream of traverse injection described earlier. Those movements, however, are not part of a large-scale streamwise vorticity field, as was the case in traverse injection. Supersonic flows do not allow for the build-up of such fields. Nevertheless, oblique injection has been proven in the literature to provide superior performance over traverse injection from the mixing point- of-view.[5] This is due to the fact that the "dips" and "bumps" induced in the shear layer generate expansion, compression, and shock waves in the airflow, which then further interact with the shear layer to provide better mixedness.

IV. Conclusions

Oblique injection of fuel in a supersonic combustor was investigated numerically in this study. The effects of important flow and injection parameters were examined for substantiation, so that the associated benefits can be utilized. These parameters include airflow pressure and Mach number, fuel pressure and mass flow rate, and injection angle. The results have shown that air static pressure is the key parameter governing mixedness in the oblique-injection flowfield. Higher pressures increase the ability of airflow to resist penetration and suppress the fuel flow to thinner boundary layers that mix up faster with air due to subsequent shock/shear layer interactions. Air Mach number does not govern the quality of air-fuel mixing, i.e., increasing air Mach number does not necessarily result in better mixedness. The increase in fuel pressure (mass flow rate) at constant airflow results in deeper penetration into the airflow but at the expense of both fuel dispersion and airflow total pressure. Under such conditions poorer mixing and higher total pressure losses were observed. Changing the injection angle (limited to small angles of up to about 20°) does not affect the flowfield significantly. The flowfield downstream of an oblique-injection port is entirely supersonic and free of boundary-layer separation and large-scale streamwise vorticity fields, unlike that of a traverse-injection port.

Acknowledgments

This work was supported by the Space Vehicle Technology Institute under grant NCC3-989 jointly funded by NASA and DoD within the NASA Constellation University Institutes Project, with Claudia Meyer as the Project Manager. The DoD work was supported by the USAF. This support is gratefully acknowledged.

The simulation code and visualization interface, ESI-CFD, was provided by ESI-Group. This support is gratefully acknowledged.

References

[1]Gruber, M.R., Nejad, A.S., Chen, T.H., and Dutton, J.C., "Mixing and Penetration Studies of Sonic Jets in a Mach 2 Freestream," Journal of Propulsion and Power, Vol. 11, No. 2, March-April 1995.

[2]Kutschenreuter, P., "Supersonic Flow Combustors," Scramjet Propulsion, edited by Curran, E.T. and Murphy,

S.N.B., Progress in Astronautics and Aeronautics Series, Vol. 189, 2000, pp. 513 – 567.

[3]Sung, C. J., Li, J. G., Yu, G., and Law, C. K., "Chemical Kinetics and Self-Ignition in a Model Supersonic Hydrogen–Air Combustor," AIAA Journal, Vol. 37, No. 2, February 1999, pp. 208 – 214.

[4]Conaire, M. O., Curran, H. J., Simmie, J. M., Pitz, W. J., and Westbrook, C. K., "A Comprehensive Modeling Study of Hydrogen Oxidation," International Journal of Chemical Kinetics, Vol. 36, Issue 11, pp. 603 – 622.

[5]Abdelhafez, A., Gupta, A. K., Balar, R., and Yu, K., "Evaluation of Oblique and Traverse Fuel Injection in a Supersonic Combustor," 43rd AIAA/ASME/SAE/ASEE Joint Propulsion Conference & Exhibit, Cincinnati, OH, July 8-11, 2007, AIAA-2007-5026

[6]Ben-Yakar, A., "Experimental Investigation of Transverse Jets in Supersonic Cross-flows," Ph.D. Dissertation, Dept. of Mechanical Eng., Stanford Univ., Stanford, CA, Dec. 2000.

[7]Huber, P. W., Schexnayder, C. J., and McClinton, C. R., "Criteria for Self-Ignition of Supersonic Hydrogen-Air Mixtures," NASA TP 1457, 1979.

[8]Ben-Yakar, A., and Hanson, R. K., "Experimental Investigation of Flame-Holding Capability of a Transverse Hydrogen Jet in Supersonic Cross-Flow," Proc. Twenty-Seventh Symposium (Intl.) on Combustion, The Combustion Inst., Pittsburgh, PA, 1998, pp. 2173 – 2180.

[9]Lee, S. H., "Characteristics of Dual Transverse Injection in Scramjet Combustor," Journal of Propulsion and Power, Vol. 22, No. 5, September–October 2006, pp. 1012 – 1019.

[10]Sunami, T., Itoh, K., Sato, K., Komuro, T., and Hashimoto, T., "Observation of the Processes of Ignition and Combustion Flowfield Formation in a Supersonic Combustor with Presence of Streamwise Vortices," AIP Second International Conference on Flow Dynamics, May 5, 2006, Vol. 832, pp. 467-480.

[11]Sunami, T., Itoh, K., Sato, K., and Komuro, T., "Mach 8 Ground Tests of the Hypermixer Scramjet for HyShot-IV Flight Experiment," 14th AIAA/AHI Space Planes and Hypersonic Systems and Technologies Conference, AIAA 2006-8062.

[12]Huh, H., and Driscoll, J. F., "Measured Effects of Shock Waves on Supersonic Hydrogen-Air Flames," 32nd Joint Propulsion Conference and Exhibit, Lake Buena Vista, FL, July, 1996, AIAA- 96-3035.

[13]Yang, J., Kubota, T., and Zukoski, E. E., "Applications of Shock-Induced Mixing to Supersonic Combustion," AIAA Journal, Vol. 31, No. 5, May 1993, pp. 854 – 862.

[14]Menon, S., "Shock-wave-induced mixing enhancement in scramjet combustors," AIAA 27th Aerospace Sciences Meeting, Reno, NV, Jan 1989, AIAA-89-0104.

[15]Balar, R., Young, G., Pang, B., Gupta, A. K., Yu, K. H., and Kothari, A. P., "Comparison of Parallel and Normal Fuel Injection in a Supersonic Combustor," 42nd AIAA/ASME/SAE/ASEE Joint Propulsion Conference and Exhibit, Sacramento, CA, July 9-12, 2006, AIAA-2006-4442.

[16]Abdelhafez, A. and Gupta, A. K., "Mixture Fraction Measurement in the Flowfield from a Coaxial Injector," 46th AIAA Aerospace Sciences Meeting and Exhibit, Reno, NV, January 7-10, 2008, AIAA-2008-0954.